

Infrared Intensities, Atomic Charges, and Dipole Moments in the Fluoroethane Series Using Atomic Polar Tensor Analysis

S. Tai, K. H. Illinger,* and S. Papasavva

Department of Chemistry, Tufts University, Medford, Massachusetts 02155

Received: June 12, 1997; In Final Form: October 8, 1997[Ⓢ]

To gain insight into the interpretation of the atomic polar tensors (APT) in the series of fluoroethanes, the fluorine, carbon, and hydrogen APT components $\mathbf{P}_\alpha^{\text{ss}'}$ were calculated, in the inertial-axes coordinate system, and examined by determining the mean dipole derivatives \bar{p}_α , the King effective atomic charges χ_α , and APT anisotropies β_α . From this, relationships between chemical bonding environment and \bar{p}_α terms are clearly discernible, with the carbon-atom charges exhibiting a labile response to the degree and form of fluorine substitution. We examine the dependence of the total absolute infrared intensities, as predicted by the APT sum rules, on the degree of fluorine substitution and molecular structure for the entire set of fluoroethanes. Finally, dipole-moment components were calculated (i) directly from *ab initio* methods at the MP2/6-31G** level, (ii) from the $\mathbf{P}_\alpha^{\text{ss}'}$ terms, and (iii) as the first moments of the \bar{p}_α atomic charges at the nuclear equilibrium positions, and a detailed comparison was made.

Introduction

We have recently been investigating trends in the absolute infrared intensities of a series of hydrofluorocarbons (HFC) and hydrochlorofluorocarbons (HCFC) using *ab initio* molecular orbital calculations,^{1–3} which provide both the wavefunction and the energy of a molecule in a given electronic state. Trends in structurally related molecules, such as in the series of interest, can also be found in the atomic charges, ζ_α , or electron population of a given atom α , derived from these wavefunctions.

The most common approach to atomic charges has been the Mulliken population analysis^{4,5} for net atomic populations, bond overlap populations, and effective charges. However, a limitation to this approach is that these measures often reflect the properties of the basis sets used rather than the details of the electron distributions themselves. Another approach to atomic charges that is more applicable to the understanding of absolute infrared intensities is atomic polar tensor (APT) analysis, which operates within the harmonic-oscillator linear dipole-moment (HO-LDM) approximation. APT analysis allows the interpretation of absolute infrared intensities in terms of the mean dipole-derivative atomic charges,^{6,7} \bar{p}_α , the mass-weighted square effective charges, (χ_α^2/m_α) , and associated King effective atomic charges, χ_α . Here m_α is the atomic mass of atom α . One of the strengths of APT analysis is that trends in a series of structurally related molecules, if they exist, will be discernible in terms of the role played by atoms of each type.

In this paper, to gain insight into the nature of atomic polar tensors in the series of fluoroethanes, we calculate the fluorine, carbon, and hydrogen APTs in the inertial-axes coordinate system, and interpret them by examining the effective atomic charges, χ_α , the mean dipole derivatives, \bar{p}_α , and the APT anisotropies β_α . Dipole moment components, μ_s^0 , $s = (x, y, z)$, are calculated (i) directly from *ab initio* methods,^{8,9} (ii) from the APT terms,^{10–12} and (iii) from the charges given by \bar{p}_α . We further develop a relationship between the degree of fluorine substitution on carbon and the charges on individual carbon, fluorine, and hydrogen atoms, and examine the dependence of the total calculated absolute infrared intensities on molecular

structure and the degree of substitution, for the entire set of fluoroethanes.

Background

In the APT method, the components $\mathbf{P}_\alpha^{\text{ss}'}$ of the atomic polar tensor \mathbf{P}_α of atom α are defined as the first derivatives of the components μ_s of the molecular dipole moment, with respect to the atomic Cartesian displacement coordinates s_α' , computed here in the inertial axes reference frame, where the s are the space-fixed Cartesian coordinates,

$$\mathbf{P}_\alpha^{\text{ss}'} = (\partial\mu_s/\partial s_\alpha') \quad (1)$$

Although the components of \mathbf{P}_α are not invariant with respect to rotation of the coordinate system, its trace is invariant.^{13–15} The mean dipole-derivative for each atom, \bar{p}_α , is defined as the trace of the $\mathbf{P}_\alpha^{\text{ss}'}$ matrix:¹³

$$\bar{p}_\alpha = (1/3) \sum_s \mathbf{P}_\alpha^{\text{ss}} \quad (2)$$

A related quantity, the King effective atomic charge, χ_α , is given by:^{6,16}

$$\chi_\alpha^2 = (1/3) \sum_{\text{ss}'} (\mathbf{P}_\alpha^{\text{ss}'})^2 \quad (3)$$

The charge χ_α and the anisotropy, β_α , of the atomic polar tensor \mathbf{P}_α are related as follows:

$$\chi_\alpha^2 = (\bar{p}_\alpha)^2 + (2/9)\beta_\alpha^2 \quad (4)$$

with

$$\beta_\alpha^2 = 1/2 [(\mathbf{P}_\alpha^{\text{xx}} - \mathbf{P}_\alpha^{\text{yy}})^2 + (\mathbf{P}_\alpha^{\text{yy}} - \mathbf{P}_\alpha^{\text{zz}})^2 + (\mathbf{P}_\alpha^{\text{zz}} - \mathbf{P}_\alpha^{\text{xx}})^2 + 3 \sum_{s \neq s'} (\mathbf{P}_\alpha^{\text{ss}'})^2] \quad (5)$$

An impediment to the interpretation of χ_α as the atomic charge, ζ_α , is that, in general, for neutral molecules, the sum of such atomic charges will not vanish. Thus, \bar{p}_α has been the preferred definition of atomic charge from APT analysis. Since these atomic charges \bar{p}_α represent the redistribution of the electronic charge density around each atom on going from the

[Ⓢ] Abstract published in *Advance ACS Abstracts*, December 1, 1997.

separated atoms to the atoms in the molecular bonding environment at the equilibrium geometry, their sum over all atoms for a neutral molecule will be equal to zero. One of the key differences between APT charges and the Mulliken charges, alluded to earlier, is that the basis-set dependence of the former arises only from the fact that the basis set can be incomplete; hence, as the basis set approaches completeness, the APT charges approach a well-defined limit.^{14,17,18}

Equilibrium dipole moment components μ_s^0 can be estimated from atomic charges, ζ_α , using the definition of the first moment of a set of atomic charges ζ_α at the nuclear equilibrium positions s_α^0 :

$$\mu_s^0 = \sum_\alpha \zeta_\alpha s_\alpha^0 \quad (6)$$

Comparison of μ_s^0 terms so computed to experiment serves as a criterion^{11,17,19} for the quality of the atomic charges ζ_α .

The equilibrium dipole-moment components μ_s^0 are rigorously expressible through the APT terms computed in the inertial-axes reference frame by:^{10–12}

$$\begin{bmatrix} 0 & \mu_z^0 & -\mu_y^0 \\ -\mu_z^0 & 0 & \mu_x^0 \\ \mu_y^0 & -\mu_x^0 & 0 \end{bmatrix} = \sum_\alpha \mathbf{P}_\alpha \rho_\alpha^0 \quad (7)$$

where

$$\rho_\alpha^0 = \begin{bmatrix} 0 & z_\alpha^0 & -y_\alpha^0 \\ -z_\alpha^0 & 0 & x_\alpha^0 \\ y_\alpha^0 & -x_\alpha^0 & 0 \end{bmatrix} \quad (8)$$

The absolute infrared intensity sum over all normal modes k for a molecule is related to the sum of the N mass-weighted square effective atomic charges through the sum rule:^{6,7,10,16,20–22}

$$\sum_{\alpha=1}^N (3\chi_\alpha^2/m_\alpha) = (N_0\pi/3c^2)^{-1} \left[\sum_{k=1}^{3N-6} \Gamma_k \nu_k^0 + \Omega + (3q^2/\sum_\alpha m_\alpha) \right] \quad (9)$$

Here, the Γ_k are the Crawford band intensity terms; Ω is the rotational correction, and the final term on the rhs is the translational correction, to the vibrational sum rule. N_0 is the Avogadro number and c is the velocity of light *in vacuo*, m_α is the atomic mass in amu, q is the molecular charge, and N is the total number of atoms. The rotational correction Ω is given by:^{6,10,16,23}

$$\Omega = [(\mu_x^0)^2 + (\mu_y^0)^2]/I_{zz} + [(\mu_y^0)^2 + (\mu_z^0)^2]/I_{xx} + [(\mu_z^0)^2 + (\mu_x^0)^2]/I_{yy} \quad (10)$$

In eq 10, I_{xx} , I_{yy} , and I_{zz} ($I_{xx} < I_{yy} < I_{zz}$), are the principal moments of inertia about the axes s ; Ω is the total absolute intensity of the pure rotational spectrum of the molecule. The Crawford band intensity terms Γ_k and harmonic frequencies ν_k^0 in eq 9 are related to the Wilson band intensity terms A_k and band-center frequencies ν_k by:^{24,25}

$$\Gamma_k \nu_k^0 = A_k (\nu_k^0/\nu_k) = (N_0\pi/3c^2) \sum_s (\partial\mu_s/\partial Q_k)_0^2 \quad (11)$$

Here, $(\partial\mu_s/\partial Q_k)_0$ is the dipole-moment derivative with respect to the normal coordinate Q_k . As a result, the infrared intensity sum in eq 9 becomes:

$$\sum_{k=1}^{3N-6} \Gamma_k \nu_k^0 = \sum_{k=1}^{3N-6} A_k (\nu_k^0/\nu_k) \cong \sum_{k=1}^{3N-6} A_k = A_{\text{tot}} \quad (12)$$

since $(\nu_k^0/\nu_k) \cong 1$. Bandshape information is required in the definition^{23,24} of the band-center frequency, $\nu_k = \int \mathcal{A}_k(\nu) d\nu / \int \mathcal{A}_k(\nu) d \ln \nu$, where $A_k = \int \mathcal{A}_k(\nu) d\nu$. In the absence of such information, comparison of computed and experimental A_k terms requires the assumption $(\nu_k^0/\nu_k) = 1$. The term A_{tot} on the rhs of eq 12 is introduced as compressed notation for the sum over all the modes k .

Equation 9 is an analog, for the interaction between an electromagnetic field and nuclear motions, of the Kuhn–Thomas sum rule for electronic motion.^{23,26–28} Equations 1, 3, and 7–12 provide a consistent framework relating the APT terms to the equilibrium molecular dipole moment and the dipole-allowed vibrational and pure-rotational intensity sums. For neutral molecules, and in the limit, $\Omega \ll A_{\text{tot}}$, eqs 4, 9, and 12 suggest a physical relationship between A_{tot} and trends in the King effective charges, χ_α , which are in turn related to the mean dipole derivatives \bar{p}_α . Employing this relationship, we shall obtain an explicit sum rule for A_{tot} , on the basis of halogen substitution and structure, for the series of fluoroethanes.

Methodology

Atomic polar tensor calculations were performed with Gaussian-92 software using four DEC ALPHA workstations. Gaussian-92 employs the HO-LDM approximation to compute the harmonic frequencies, ν_k^0 , and absolute intensities, A_k , of the fundamental transitions of each normal mode of vibration k , as well as the atomic polar tensors, \mathbf{P}_α . Second-order Møller–Plesset perturbation theory and the 6-31G** basis set (MP2/6-31G**) were used. This has been found to provide reasonable representations of properties of molecules of the type considered here.^{1–3} At this level of theory, the atomic coordinates, s_α^0 , should be given to good accuracy, as attested to by the accuracy of the calculated molecular geometries. The entire series (excluding ethane) of $\text{CH}_3\text{-}_n\text{F}_n\text{CH}_3\text{-}_n'\text{F}_n'$ ($n\text{F}$, $n\text{F}' = 0, 1, 2, 3$) was examined, and optimized geometries (without symmetry constraints) were found. For the unclustered compounds ($n\text{F} - n\text{F}' \leq 1$, where $n\text{F} + n\text{F}' = 2, 3, 4$), geometries were optimized for both the anti and gauche conformations. In addition, four chlorinated ethanes were examined: CF_2ClCH_3 , CFCl_2CH_3 , CHCl_2CF_3 , and CHClCF_3 (the latter computed with MP2/6-31G*). Optimized geometries and other molecular properties, including the I_{ss} terms required in eq 10, have been presented in previous papers;^{1–3} the atomic polar tensors \mathbf{P}_α used in our computations are available.^{3a}

Results and Discussion

Atomic Charges. The mean dipole-derivative atomic charges, \bar{p}_α ; the King effective atomic charges, χ_α ; APT anisotropies, β_α ; dipole-moment components, $(\mu_s^0)_{\text{APT}}$, computed with eq 7; dipole-moment components, $(\mu_s^0)_p$, computed with eq 6; total intensities, A_{tot} , eq 12; and rotational corrections, Ω , computed, eq 10, with the $(\mu_s^0)_{\text{APT}}$, are presented in Tables 1–3. To permit direct comparison with these quantities from APT analysis, we cite the $(\mu_s^0)_{\text{comp}}$ and the $(\mu_s^0)_{\text{exp}}$ (where available) and $(\mu^0)_{\text{exp}}$ previously tabulated.² The assumption made in the above, $\Omega \ll A_{\text{tot}}$, is borne out for the entire set of molecules studied here, as expected in the limit of large I_{ss} values, with a maximum deviation of <5%, within the computational or experimental errors of total absolute infrared intensities.

The \bar{p}_α values reflect what one would anticipate from physical reasoning, with the average charges $\langle \bar{p}_F \rangle$ and $\langle \bar{p}_H \rangle$ for the set

TABLE 1: Mean Dipole Derivatives, \bar{p}_α , eq 2; King Effective Charges, χ_α , eq 3; and APT Anisotropies, β_α , eq 5 of Clustered HFCs, in e. Experimental Dipole-Moment Components, $(\mu_s^0)_{\text{exp}}$; Dipole-Moment Components, $(\mu_s^0)_{\text{APT}}$, Computed with eq 7; and Dipole-Moment Components, $(\mu_s^0)_p$, Computed with eqs 2 and 6, in D. Total *ab Initio* Absolute Infrared Intensities, A_{tot} , eqs 11 and 12, and Rotational Corrections, Ω , eq 10, Computed with the $(\mu_s^0)_{\text{APT}}$ Terms, in km mol^{-1}

CH ₃ CH ₂ F (HFC 161)				CHF ₂ CH ₃ (HFC 152a)				CF ₃ CH ₃ (HFC 143a)						
	\bar{p}_α	χ_α	β_α		\bar{p}_α	χ_α	β_α		\bar{p}_α	χ_α	β_α			
C1	0.635	0.673	0.47	C2	1.144	1.165	0.44	C2	1.600	1.600	0.03			
C2	0.007	0.086	0.18	C1	-0.057	0.142	0.22	C1	-0.080	0.144	0.25			
F1	-0.488	0.562	0.59	F1	-0.523	0.599	0.34	F1	-0.536	0.606	0.60			
H4	-0.067	0.109	0.18	F2	-0.523	0.599	0.34	F2	-0.536	0.606	0.60			
H5	-0.067	0.109	0.18	H1	-0.085	0.112	0.14	F3	-0.536	0.606	0.60			
H1	-0.006	0.081	0.17	H2	0.012	0.071	0.08	H1	0.029	0.065	0.12			
H2	-0.007	0.083	0.18	H3	0.018	0.067	0.13	H2	0.029	0.065	0.12			
H3	-0.006	0.081	0.17	H4	0.012	0.071	0.08	H3	0.029	0.065	0.12			
	comp	APT	\bar{p}	exp	comp	APT	\bar{p}	exp	comp	APT	\bar{p}	exp		
μ_x^0	-1.72	-1.49	-2.47	1.69	μ_x^0	-2.07	-1.78	-3.24	2.07	μ_x^0	2.44	2.23	4.08	
μ_y^0	1.18	1.00	1.75	1.00	μ_y^0	0.00	0.00	0.00	0.00	μ_y^0	0.00	0.00	0.00	
μ_z^0	0.00	0.00	0.00	0.00	μ_z^0	1.20	0.99	2.04	1.20	μ_z^0	0.00	0.00	0.00	
μ^0	2.09	1.80	3.02	1.96	μ^0	2.39	2.04	3.83	2.30	μ^0	2.44	2.23	4.08	2.32
	Ω	A_{tot}			Ω	A_{tot}			Ω	A_{tot}				
	7	282			5	520			4	831				
CF ₃ CFH ₂ (HFC 134a)				CHF ₂ CF ₃ (HFC 125)				CF ₃ CF ₃ (HFC 116)						
	\bar{p}_α	χ_α	β_α		\bar{p}_α	χ_α	β_α		\bar{p}_α	χ_α	β_α			
C2	1.539	1.541	0.14	C2	1.498	1.505	0.31	C1	1.487	1.495	0.33			
C1	0.477	0.544	0.25	C1	1.008	1.042	0.56	C2	1.487	1.495	0.33			
F1	-0.519	0.589	0.32	F1	-0.507	0.576	0.58	F1	-0.496	0.565	0.57			
F2	-0.519	0.589	0.32	F2	-0.505	0.575	0.58	F2	-0.496	0.565	0.57			
F3	-0.521	0.590	0.39	F3	-0.507	0.576	0.58	F3	-0.496	0.565	0.57			
F4	-0.430	0.496	0.35	F4	-0.475	0.547	0.58	F4	-0.496	0.565	0.57			
H1	-0.013	0.059	0.06	F5	-0.475	0.547	0.58	F5	-0.496	0.565	0.57			
H2	-0.013	0.059	0.06	H1	-0.037	0.058	0.10	F6	-0.496	0.565	0.57			
	comp	APT	\bar{p}	exp	comp	APT	\bar{p}	exp	comp	APT	\bar{p}	exp		
μ_x^0	-0.43	-0.35	-1.14	0.41	μ_x^0	-0.26	-0.20	-0.64	μ_x^0	0.00	0.00	0.00		
μ_y^0	2.24	1.84	3.49	1.75	μ_y^0	0.00	0.00	0.00	μ_y^0	0.00	0.00	0.00		
μ_z^0	0.00	0.00	0.00	0.00	μ_z^0	-1.76	-1.45	-3.07	μ_z^0	0.00	0.00	0.00		
μ^0	2.28	1.87	3.67	1.80	μ^0	1.78	1.46	3.13	1.54	μ^0	0.00	0.00	0.00	
	Ω	A_{tot}			Ω	A_{tot}			Ω	A_{tot}				
	2	867			1	1070			0	1383				

^a Sources of $(\mu_s^0)_{\text{exp}}$ in this comparison are available in ref 2.

being -0.489 e and -0.033 e, respectively. The carbon charges display a marked sensitivity to the bonding environment (ranging from -0.064 to 1.626 e), in contrast to the more electronegative fluorines (ranging only from -0.542 to -0.436 e), or the nearly-neutral hydrogens (ranging from -0.091 to 0.026 e). We estimate the relative error to be ± 0.0001 e in the \bar{p}_α and χ_α terms, and ± 0.0003 e in β_α . These error estimates were obtained by taking the maximum deviation between computed values for sets of atoms that are equivalent by symmetry, in the optimized geometry.

Our computed fluorine charges are comparable to those found in the fluoromethane series from APTs derived from experimental intensities²⁹⁻³² (-0.531 , -0.524 , -0.500 , and -0.474 e for CF₄, CHF₃, CH₂F₂, and CH₃F) and from computationally determined³³ APTs (-0.374 , -0.380 , -0.404 , and -0.434 e for CF₄, CHF₃, CH₂F₂, and CH₃F). In addition, the calculated \bar{p}_F , χ_F , and β_F for C₂F₆ in this paper (-0.496 , 0.565 , and 0.574 e, respectively) are comparable³² to those found from APTs derived from experimental intensities (-0.443 , 0.505 , and 0.686 e, respectively) and from computationally determined APTs (-0.522 , 0.550 , and 0.371 e, respectively). The difference in computed values probably arises from differences in level of theory and basis set (HF/4-31G for ref 32).

As seen in Figure 1a, we find a strong regularity in the relationship between atomic charges \bar{p}_C in the set of fluoro-

ethanes and the chemical environment (specifically, fluorine substitution). Similar regularities, but with a strongly attenuated response, can be seen for \bar{p}_F , Figure 1b, and \bar{p}_H , Figure 1c. When a linear regression analysis is performed relating \bar{p}_α as a dependent variable to the independent variables, nF and nF' , one obtains expressions for \bar{p}_C , \bar{p}_F , and \bar{p}_H . Since for a neutral molecule, $\sum_\alpha \bar{p}_\alpha = 0$, we have used the maximum computed deviation (0.01 e) of the regression sums from zero as a measure of the standard error of our regression lines. The latter are found to be:

$$\bar{p}_C = 0.08 + 0.52nF - 0.05nF' \quad R^2 = 0.998$$

$$\bar{p}_F = -0.46 - 0.03nF + 0.02nF' \quad R^2 = 0.955$$

$$\bar{p}_H = -0.03 - 0.03nF + 0.02nF' \quad R^2 = 0.973 \quad (13)$$

From the coefficients of the regression lines in eq 13, the effects of varying degrees of fluorine substitution on the atomic charges \bar{p}_α can clearly be seen. While nF has a stronger influence than nF' , in general, the effect that fluorine substitution has on \bar{p}_F and \bar{p}_H is relatively small. In contrast to this, because of the high electronegativity of fluorine, increasing substitution on carbon by fluorine serves to increase \bar{p}_C significantly, while increasing substitution on the neighboring carbon atom by

TABLE 2: Mean Dipole Derivatives, \bar{p}_α , eq 2; King Effective Charges, χ_α , eq 3; and APT Anisotropies, β_α , eq 5 of Unclustered HFCs, in e. Experimental Dipole-Moment Components, $(\mu_s^0)_{\text{exp}}$; Dipole-Moment Components, $(\mu_s^0)_{\text{APT}}$, Computed with eq 7; and Dipole-Moment Components, $(\mu_s^0)_p$, Computed with eqs 2 and 6, in D. Total *ab Initio* Absolute Infrared Intensities, A_{tot} , eqs 11 and 12, and Rotational Corrections, Ω , Equation 10, Computed with the $(\mu_s^0)_{\text{APT}}$ Terms, in Km mol^{-1}

CH ₂ FCH ₂ F (HFC 152)				CH ₂ FCHF ₂ (HFC 143)				CHF ₂ CHF ₂ (HFC 134)			
\bar{p}_α	χ_α	β_α	anti	\bar{p}_α	χ_α	β_α	anti	\bar{p}_α	χ_α	β_α	anti
C2	0.552	0.598	0.49	C2	1.068	1.095	0.51	C2	1.019	1.058	0.60
C1	0.552	0.598	0.49	C1	0.494	0.563	0.57	C1	1.019	1.058	0.60
F1	-0.461	0.528	0.55	F1	-0.501	0.573	0.59	F1	-0.486	0.559	0.59
H1	-0.046	0.085	0.15	F2	-0.504	0.580	0.61	F2	-0.486	0.559	0.59
H2	-0.046	0.085	0.15	H1	-0.063	0.085	0.12	H1	-0.047	0.067	0.10
F2	-0.461	0.528	0.55	F3	-0.444	0.511	0.54	F3	-0.486	0.559	0.59
H3	-0.046	0.085	0.15	H2	-0.028	0.073	0.14	F4	-0.486	0.559	0.59
H4	-0.046	0.085	0.15	H3	-0.022	0.063	0.13	H2	-0.047	0.067	0.10
comp	APT	\bar{p}	exp	comp	APT	\bar{p}	exp	comp	APT	\bar{p}	exp
μ_x^0	0.00	0.00	0.00	μ_x^0	-0.21	-0.17	-0.62	μ_x^0	0.00	0.00	0.00
μ_y^0	0.00	0.00	0.00	μ_y^0	-1.69	-1.42	-2.60	μ_y^0	0.00	0.00	0.00
μ_z^0	0.00	0.00	0.00	μ_z^0	0.48	0.39	0.95	μ_z^0	0.00	0.00	0.00
μ^0	0.00	0.00	0.00	μ^0	1.77	1.49	2.84	μ^0	0.00	0.00	0.00
Ω	A_{tot}			Ω	A_{tot}			Ω	A_{tot}		
0	345			2	558			0	764		
CH ₂ FCH ₂ F (HFC 152)				CH ₂ FCHF ₂ (HFC 143)				CHF ₂ CHF ₂ (HFC 134)			
\bar{p}_α	χ_α	β_α	gauche	\bar{p}_α	χ_α	β_α	gauche	\bar{p}_α	χ_α	β_α	gauche
C1	0.555	0.610	0.54	C2	1.083	1.105	0.47	C2	1.029	1.059	0.53
C2	0.555	0.610	0.54	C1	0.505	0.564	0.53	C1	1.029	1.059	0.53
F1	-0.467	0.539	0.57	F1	-0.504	0.577	0.60	F1	-0.487	0.559	0.58
H1	-0.048	0.094	0.17	F2	-0.504	0.577	0.60	F2	-0.489	0.561	0.58
H2	-0.039	0.080	0.15	H1	-0.072	0.099	0.14	H1	-0.053	0.076	0.12
F2	-0.467	0.539	0.57	F3	-0.446	0.512	0.54	F3	-0.487	0.559	0.58
H3	-0.048	0.093	0.17	H2	-0.031	0.075	0.15	F4	-0.489	0.561	0.58
H4	-0.039	0.080	0.15	H3	-0.031	0.075	0.15	H2	-0.053	0.076	0.12
comp	APT	\bar{p}	exp	comp	APT	\bar{p}	exp	comp	APT	\bar{p}	exp
μ_x^0	0.00	0.00	0.00	μ_x^0	0.26	0.23	0.49	μ_x^0	0.00	0.00	0.00
μ_y^0	3.06	2.61	4.45	μ_y^0	0.00	0.00	0.00	μ_y^0	0.00	0.00	0.00
μ_z^0	0.00	0.00	0.00	μ_z^0	3.58	3.01	5.60	μ_z^0	-2.79	-2.31	-4.71
μ^0	3.06	2.61	4.45	μ^0	3.59	3.02	5.62	μ^0	2.79	2.31	4.71
Ω	A_{tot}			Ω	A_{tot}			Ω	A_{tot}		
12	347			9	571			4	769		

^a Sources of $(\mu_s^0)_{\text{exp}}$ in this comparison are available in ref 2, and that for CH₂FCH₂F, in ref 41.

TABLE 3: Mean Dipole Derivatives, \bar{p}_α , eq 2; King Effective Charges, χ_α , eq 3; and APT Anisotropies, β_α , eq 5 of the HCFCs, in e. Experimental Dipole-Moment Components, $(\mu_s^0)_{\text{exp}}$; Dipole-Moment Components, $(\mu_s^0)_{\text{APT}}$, Computed with eq 7; and Dipole-Moment Components, $(\mu_s^0)_p$, Computed with eqs 2 and 6, in D. Total *ab Initio* Absolute Infrared Intensities, A_{tot} , eqs 11 and 12 and Rotational Corrections, Ω , eqs 10, Computed with the $(\mu_s^0)_{\text{APT}}$ Terms, in km mol^{-1}

CF ₂ ClCH ₃ (HCFC 142b)				CFCl ₂ CH ₃ (HCFC 141b)				CHClFCF ₃ (HCFC 124)				CHCl ₂ CF ₃ (HCFC 123)			
\bar{p}_α	χ_α	β_α		\bar{p}_α	χ_α	β_α		\bar{p}_α	χ_α	β_α		\bar{p}_α	χ_α	β_α	
C2	1.476	1.506	0.64	C2	1.285	1.285	0.73	C2	1.509	1.515	0.27	C2	1.507	1.514	0.30
C1	-0.090	0.145	0.24	C1	-0.092	0.092	0.18	C1	0.784	0.893	0.90	C1	0.523	0.714	1.03
F1	-0.550	0.625	0.63	F1	-0.552	0.552	0.59	F1	-0.530	0.613	0.65	F1	-0.520	0.594	0.61
F2	-0.550	0.625	0.63	C11	-0.360	0.360	0.60	F2	-0.502	0.563	0.54	F2	-0.520	0.594	0.61
C11	-0.369	0.467	0.61	C12	-0.360	0.360	0.60	F3	-0.497	0.560	0.55	F3	-0.490	0.548	0.52
H1	0.032	0.062	0.11	H1	0.023	0.023	0.13	F4	-0.470	0.554	0.62	C11	-0.247	0.325	0.45
H2	0.032	0.062	0.11	H2	0.033	0.033	0.11	C11	-0.269	0.345	0.46	C12	-0.247	0.325	0.45
H3	0.019	0.069	0.14	H3	0.023	0.023	0.13	H1	-0.027	0.059	0.11	H1	-0.006	0.058	0.12
comp	APT	\bar{p}	exp	comp	APT	\bar{p}	exp	comp	APT	\bar{p}	exp	comp	APT	\bar{p}	exp
μ_x^0	1.06	1.03	1.30	μ_x^0	0.00	0.00	0.00	μ_x^0	0.38	0.23	1.27	μ_x^0	-0.44	-0.26	-1.57
μ_y^0	2.14	1.81	3.63	μ_y^0	1.59	1.47	2.21	μ_y^0	-0.07	-0.02	-0.30	μ_y^0	0.00	0.00	0.00
μ_z^0	0.00	0.00	0.00	μ_z^0	-1.60	-1.34	-2.76	μ_z^0	-1.64	-1.37	-2.64	μ_z^0	-1.45	-1.29	-2.12
μ^0	2.39	2.09	3.85	μ^0	2.26	1.99	3.53	μ^0	1.68	1.39	2.94	μ^0	1.51	1.32	2.64
Ω	A_{tot}			Ω	A_{tot}			Ω	A_{tot}			Ω	A_{tot}		
3	729			2	562			1	975			1	864		

fluorine decreases \bar{p}_C slightly. From the regression fit, it is evident that each additional fluorine on carbon contributes $\sim +0.52$ e to the carbon charge. This is comparable to the results of Ferreira and Suto³³ who find that each additional fluorine adds approximately 0.5 e to the carbon charge in the

substituted methanes. Similar carbon charge changes have been found³¹ in fluoromethanes. Although the effect is small, \bar{p}_F becomes slightly more negative as nF increases.

For neutral molecules, the sum of the \bar{p}_α terms over all atoms vanishes.^{6,13,16,21,34} In the set of molecules examined here, the

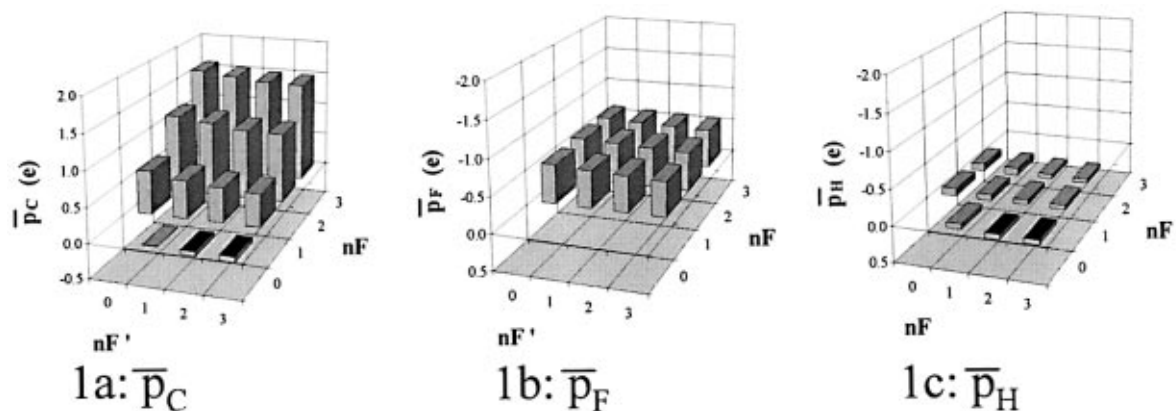


Figure 1. Relationship between atomic charges \bar{p}_α in the set of fluoroethanes, $\text{CH}_3\text{-}_n\text{F}_n\text{CH}_3\text{-}_n'\text{F}_{n'}$, and the chemical bonding environment, eq 13. In Figures 1a and 1c, black shading indicates the zero of the y -coordinate, for negative values of \bar{p}_α .

\bar{p}_F and \bar{p}_H terms do not show large deviations from their averages, $\langle\bar{p}_F\rangle$ and $\langle\bar{p}_H\rangle$, and we may write:

$$-(\bar{p}_C + \bar{p}_{C'}) \cong \langle\bar{p}_F\rangle [nF + nF'] + \langle\bar{p}_H\rangle [6 - (nF + nF')] \quad (14)$$

Equation 14 approximately describes the balance between the nearly constant fluorine charges, with $\langle\bar{p}_F\rangle \cong -0.49$ and $\langle\bar{p}_H\rangle \cong -0.03$, and the highly labile carbon charges, \bar{p}_C and $\bar{p}_{C'}$.

Through use of regression lines for χ_α , similar to those for \bar{p}_α , eq 13, APT analysis permits the expression of A_{tot} as a function of the contribution, $(3\chi_\alpha^2/m_\alpha)$, of each atom and the number of atoms of each type. Our regression lines for the relationship between the King effective atomic charges χ_α and fluorine substitution are as follows:

$$\chi_C = |0.10 + 0.52nF - 0.05nF'| \quad R^2 = 0.989$$

$$\chi_F = |-0.53 - 0.03nF + 0.02nF'| \quad R^2 = 0.924$$

$$\chi_H = |-0.06 - 0.04nF + 0.03nF'| \quad R^2 = 0.657 \quad (15)$$

Apart from describing the relationship between the atomic charges and the bonding environment, APT analysis of the anti and gauche conformers permits the investigation of the dependence of atomic charges on torsional angles. Some \bar{p}_α terms undergo definitive changes on going from anti to gauche, well beyond the putative relative error of $\sim\pm 0.0001$ e. Going from the higher-symmetry conformer to the lower-symmetry conformer reduces the number of atoms in equivalent bonding environments. Thus, the anti conformer of $\text{CH}_2\text{FCH}_2\text{F}$ (C_{2h}) has an equivalent set of atoms of each atomic type, with identical values of \bar{p}_α , β_α , and hence χ_α within each set, with $\bar{p}_H = -0.046$ e. Reduction of the symmetry to C_2 in the gauche form splits the hydrogen atoms into two sets, with \bar{p}_H equal to -0.039 e and -0.048 e, with HCCF torsional angles of 51° and 172° , respectively. The charges \bar{p}_C and \bar{p}_F show small positive and negative increases, respectively. The net result is a small increase in $\sum_\alpha (3\chi_\alpha^2/m_\alpha)$, on going from the anti to the gauche form, as well as a small increase in the charge difference between \bar{p}_C and \bar{p}_F on going to the gauche forms. Because larger differences between the carbon and fluorine charges lead to shorter corresponding bonds, this is consistent with the well-documented gauche effect,³⁵⁻³⁷ in which C-F bond lengths are shorter in gauche forms than in anti forms, consistent with our computed equilibrium geometries.²

In the case of CH_2FCHF_2 , since the bonding environments at C1 and C2 differ, the gauche conformer (C_s) exhibits atomic-

charge sets, [C1; (F1, F2); H1] and [C2; F3; (H2, H3)], respectively, with an HCCF torsional angle 60.5° , and all FCCF torsional angles 59.2° . On going to the anti form, with reduction of the symmetry to C_1 , the (F1, F2) and (H2, H3) components are split, with an attendant change in \bar{p}_F and \bar{p}_H , and one obtains three nonequivalent hydrogens and fluorines. In this case, $\sum_\alpha (3\chi_\alpha^2/m_\alpha)$ decreases slightly. The anti conformer of CHF_2CHF_2 (C_{2h}), again has equivalent-atom sets of each type. On going to the gauche form, C_2 , the fluorines split into two sets, analogously to the hydrogens in $\text{CH}_2\text{FCH}_2\text{F}$. The attendant changes in \bar{p}_α lead to a small increase in $\sum_\alpha (3\chi_\alpha^2/m_\alpha)$.

Implicit in the form of eq 4 is nonlinear behavior for β_α as a function of a variable upon which \bar{p}_α and χ_α depend linearly. Thus, while the mean dipole-derivative atomic charges \bar{p}_α for the fluoroethanes are monotonically varying functions of nF and nF' , the β_α terms are influenced by the bonding environment in a more complicated fashion. In particular, among the clustered species ($nF, nF' = 0, 1, 2, 3, nF - nF' \geq 2$, when $nF + nF' = 2, 3, 4$), the β_C terms for the more substituted carbon atom show a minimum for CF_3CH_3 and thence increase toward maxima at CFH_2CH_3 and CF_3CF_3 . The β_C terms for the less substituted carbon atom show a maximum for CHF_2CF_3 , descending toward minima at CH_2FCH_3 and CF_3CF_3 . Similarly, β_F in the clustered species undulates between ~ 0.3 e and ~ 0.6 e. In contrast, in the set of unclustered species, the β_C terms ($\sim 0.5\text{--}0.6$ e) do not show wide extrema, with a similar behavior for β_F ($\sim 0.55\text{--}0.6$ e). The β_H terms are fairly small throughout ($\sim 0.06\text{--}0.18$ e). In spite of this complicated behavior of the β_α terms, since the quantities \bar{p}_α constitute the dominant contribution to χ_α , eq 4, the latter also vary approximately monotonically with nF and nF' .

Among the hydrochlorofluorocarbons, we find an average charge $\langle\bar{p}_{\text{Cl}}\rangle = -0.309$ e, with a range for \bar{p}_{Cl} from -0.369 e to -0.247 e, a difference from \bar{p}_F not unexpected between chlorine and fluorine. Because of the relatively limited size of our chlorinated hydrofluorocarbon set, it is more difficult to draw definitive correlations between atomic charges and substitution than in the clearly delineated case of the fluoroethanes.

Intensity Sum Rule. The general expression for the lhs of eq 9, for the set of fluorinated ethanes is: Here, C and C' denote

$$\sum_\alpha 3(\chi_\alpha^2/m_\alpha) = 3 \{ (1/m_C)[\chi_C^2 + \chi_{C'}^2] + (1/m_F)[nF\chi_F^2 + nF'\chi_{F'}^2] + (1/m_H)[(3 - nF)\chi_H^2 + (3 - nF')\chi_{H'}^2] \} \quad (16)$$

the two individual carbons, and F and F' and H and H' denote the fluorines and hydrogens on those carbons, respectively; substituting for the χ_α using eq 15 gives a power series in nF and nF' . Molecular symmetry dictates the same coefficient for

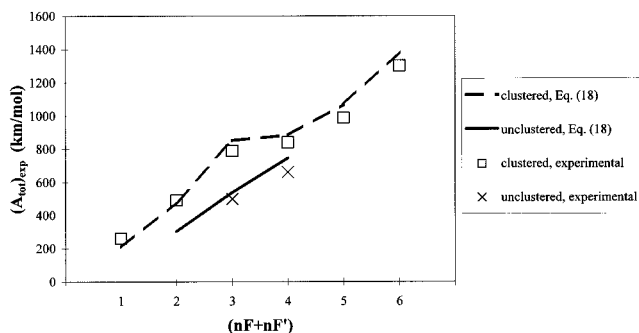


Figure 2. Experimental total absolute infrared intensity, $(A_{\text{tot}})_{\text{exp}}$, and APT absolute intensity sum, $(A_{\text{tot}})_{\text{regr}}$, eq 18, as a function of the total number of fluorines ($nF + nF'$). Sources of $(A_{\text{tot}})_{\text{exp}}$ are available in ref 2, and that for CF_3CF_3 in ref 42.

analogous terms in the power series. In consequence, the rhs of eq 16 takes on the form:

$$\sum_{\alpha} 3(\chi_{\alpha}^2/m_{\alpha}) = 3 \{c_0 + c_1(nF + nF') + c_2(nF^2 + nF'^2) + c_{11}nFnF' + c_3(nF^3 + nF'^3) + c_{12}(nF^2nF' + nF'^2nF)\} \quad (17)$$

Combining eqs 15–17, we obtain:

$$\sum_{\alpha} 3(\chi_{\alpha}^2/m_{\alpha}) = 0.066 + 0.071(nF + nF') + 0.087(nF^2 + nF'^2) - 0.057nFnF' - 0.005(nF^3 + nF'^3) + 0.005(nF^2nF' + nF'^2nF) \quad (18)$$

Equations 9, 12, and 18 permit the estimation of A_{tot} from a knowledge of the bonding environment of the molecule. When the *ab initio* terms $(A_{\text{tot}})_{\text{comp}}$ and those computed from eq 18 are compared, a strong correlation is seen, providing a fit, $(A_{\text{tot}})_{\text{comp}} = 0.942(A_{\text{tot}})_{\text{regr}} + 45$ (km mol^{-1}), with $R^2 = 0.993$. Here, $(A_{\text{tot}})_{\text{regr}} = (N_0\pi/3c^2) [\sum_{\alpha} 3(\chi_{\alpha}^2/m_{\alpha}) - \Omega]$, computed from eq 18, with $\Omega = 0$. Since clustered species exhibit considerably larger nonlinear terms ($nF^i + nF'^i$) for the same total number of fluorines ($nF + nF'$) than the unclustered species, A_{tot} is consistently larger for the former. This is a direct result of the strong dependence of the carbon charges \bar{p}_C and \bar{p}_C' on the degree of fluorine substitution, as expressed by eq 14, and the difference in the ($nF^i + nF'^i$) terms between clustered and unclustered species. Analogous arguments account for the structure dependence of the instantaneous infrared radiative forcing associated with this set of molecules.³⁸

In Figure 2 we compare $(A_{\text{tot}})_{\text{regr}}$ and the experimental terms $(A_{\text{tot}})_{\text{exp}}$ for the set of fluoroethanes, as a function of the total number of fluorines. The plateau seen in the $(A_{\text{tot}})_{\text{exp}}$ terms for the clustered species is clearly reflected in the terms calculated from eq 18. The quality of the fit of $(A_{\text{tot}})_{\text{regr}}$ to $(A_{\text{tot}})_{\text{exp}}$ for the unclustered species, with its monotone dependence on $(nF + nF')$, further corroborates the analysis.

Dipole Moments. While atomic charges are not directly accessible to experiment, the components μ_s^0 of the equilibrium dipole moments along the inertial axes are. As a result, one of the criteria for the quality of atomic charges is their accuracy in predicting the molecular dipole moment.^{11,17,19} In Tables 1 and 2, the *ab initio* dipole moments, $(\mu_s^0)_{\text{comp}}$, $(\mu_s^0)_{\text{APT}}$, from eq 7, and those from eqs 6, $(\mu_s^0)_p$, are compared with experimental dipole moments $(\mu_s^0)_{\text{exp}}$ where available.

Ideally, comparison should be made between computed dipole-moment components μ_s^0 and those from experiment. However, the paucity of the latter for the set of molecules addressed here (and generally for molecules of this level of complexity) precludes a meaningful comparison. Nonetheless, it is instructive to compare components $(\mu_s^0)_p$ computed with

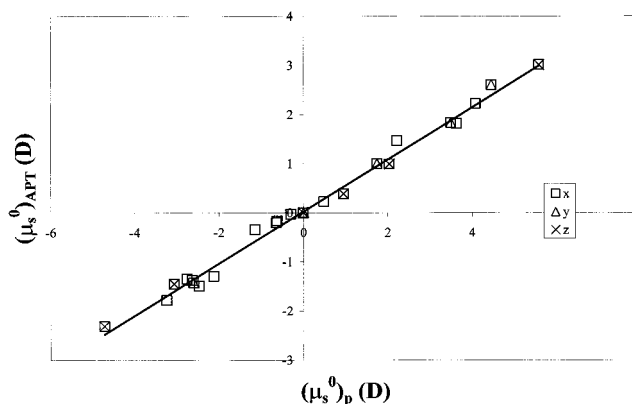


Figure 3. Combined fit of all the dipole moment components: $(\mu_s^0)_{\text{APT}}$ and $(\mu_s^0)_p$, $s = (x, y, z)$. $((\mu_s^0)_p)_{\text{regr}} = 0.530(\mu_s^0)_p + 0.023$ D, ($R^2 = 0.993$).

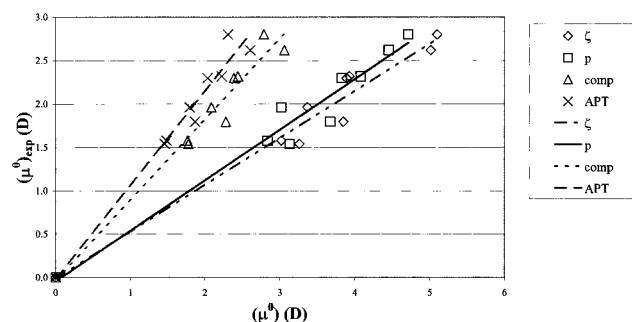


Figure 4. Comparison of calculated total dipole moments, (μ^0) , and experimental values, $(\mu^0)_{\text{exp}}$. Sources for $(\mu^0)_{\text{exp}}$ are available in ref 2, and that for 1,2-difluoroethane is available in ref 41. $((\mu^0)_p)_{\text{regr}} = 0.583(\mu^0)_p - 0.044$ D, $R^2 = 0.957$. $((\mu^0)_{\text{APT}})_{\text{regr}} = 1.077(\mu^0)_{\text{APT}} - 0.010$ D, $R^2 = 0.964$. $((\mu^0)_{\zeta})_{\text{regr}} = 0.543(\mu^0)_{\zeta} - 0.018$ D, $R^2 = 0.957$. $((\mu^0)_{\text{comp}})_{\text{regr}} = 0.922(\mu^0)_{\text{comp}} - 0.025$ D, $R^2 = 0.962$.

atomic charges \bar{p}_{α} , eqs 2 and 6, and those, $(\mu_s^0)_{\text{APT}}$, computed from eq 7, in order to examine the consistency of these different calculations of the components. The equation for the regression line, for the fluoroethanes, shown in Figure 3, is: $((\mu_s^0)_p)_{\text{regr,APT}} = 0.530(\mu_s^0)_p + 0.023$ D, ($R^2 = 0.993$). It is reassuring that the $(\mu_s^0)_p$ fit each of the $(\mu_s^0)_{\text{APT}}$ components, $s = (x, y, z)$, equally well. However, incorporating the components for all the molecules in the set in the regression may serve to suppress some variances. Not unexpectedly, inclusion of the chlorinated fluoroethanes, Table 3, in this comparison decreases R^2 by attempting to fit an additional set of atomic charges, \bar{p}_{Cl} , with a considerably more complicated, and hence more computationally challenging electron charge distribution, $\rho_{\text{el}}(x, y, z)$.

Figure 4 compares experimental total dipole moments $(\mu^0)_{\text{exp}}$ and dipole moments calculated from eq 6 using \bar{p}_{α} , $(\mu^0)_p$; using Mulliken charges, ζ_{α} , $(\mu^0)_{\zeta}$; the *ab initio* $(\mu^0)_{\text{comp}}$, and the $(\mu^0)_{\text{APT}}$. The regression equations are quoted in Figure 4. Although the *ab initio* terms are more directly comparable to experiment, there is a close linear relationship between the $(\mu^0)_{\text{APT}}$ and experiment as well, with dipole moments calculated from eq 7, on average, only slightly lower than the experimental ones. As can be seen, Mulliken and \bar{p}_{α} atomic charges routinely overestimate dipole moments. This suggests that the level of theory employed here overestimates the \bar{p}_{α} and ζ_{α} terms by roughly a factor of two. The quantum-mechanical decomposition^{6,7,11} of APTs addresses the issue of scaling ζ_{α} terms more rigorously, though not in a fashion independent of the model, but has not been applied to nonplanar molecules. We note that such previous attempts⁴⁰ to scale Mulliken charges lead, on average, to scaling factors < 1 . Critical comparisons of atomic charges obtained with different methods have been made.^{11,14,17–19}

We confine our discussion within the present context mainly to those derived from APT analysis.

The APT model makes no *a priori* assumptions concerning the decomposition of the molecular dipole moment; as a result, there is a strong correspondence between the $(\mu_s^0)_{\text{APT}}$ and $(\mu_s^0)_{\text{comp}}$ terms. Taking the trace of \mathbf{P}_α to obtain the atomic charges \bar{p}_α obliterates information, contained in the set of its components $\mathbf{P}_\alpha^{\text{ss}}$, concerning the polarization and anisotropy of the charge distribution in the vicinity of nucleus α . If the equilibrium geometry is accurate, the error introduced on going from the terms $(\mu_s^0)_{\text{APT}}$ to $(\mu_s^0)_p$ is a measure of that effect. In general, and for the APTs calculated here in the inertial-axes framework, it is not possible to define a unique correspondence between the atomic charges encountered in eqs 6 and 7, respectively.^{11,12,39} At the level of the theory employed here, barycenters of positive charge for a given molecule are closely similar for all calculations with eqs 6 and 7, irrespective of the specific choice of the measure of the electronic charge distribution $\rho_{\text{el}}(x, y, z)$, since nuclear charges are fixed and the equilibrium geometry is in good agreement with experiment. The quality of $\rho_{\text{el}}(x, y, z)$ then determines the accuracy of the barycenter of negative charge and the agreement of the computed μ_s^0 terms with experiment. As discussed above, the dipole-moment components calculated from eq 7 and those from *ab initio* differ somewhat, owing to the difference in the representation of $\rho_{\text{el}}(x, y, z)$, with the APT terms consisting of averages of the (in general, asymmetric) charge distribution in the vicinity of each nucleus, and the *ab initio* estimate not directly relying on such localized averaging.

Conclusion

We have found salient relationships between structure, degree of substitution, and atomic charges in the complete set of fluoroethanes. The atomic charges are similar to those found in previous studies on halogenated methanes. Charges on fluorine and hydrogen are seen to fall into a much narrower range than the highly labile charges on carbon, suggesting that the carbon atoms exhibit the main atomic-charge dependence on bonding environment in this systematically variegated set of structurally related molecules. From the relationships between structure, degree of substitution, and atomic charge, we are able to relate these properties to the absolute infrared intensity sum rules. Dipole moments computed directly *ab initio* or from the APT components and an accurate equilibrium nuclear geometry are in essential agreement with experiment, while those computed as first moments of APT or Mulliken atomic charges are generally overestimated.

Acknowledgment. The authors acknowledge helpful discussions with Professor J. E. Kenny of this department.

References and Notes

(1) Papasavva, S.; Tai, S.; Esslinger, A.; Illinger, K.H.; Kenny, J. E. *J. Phys. Chem.* **1995**, *99*, 3438.
 (2) Papasavva, S.; Illinger, K. H.; Kenny, J. E. *J. Phys. Chem.* **1996**, *100*, 10100. Note: In Figure 1, experimental A_{win} data were incorrectly labeled A_{tot} .

(3) Papasavva, S.; Illinger, K. H.; Kenny, J. E. *J. Mol. Struct. (THEOCHEM)* **1997**, *393*, 73. (a) Tai, S. Ph.D. Thesis, Tufts University, 1997.
 (4) Mulliken, R. S. *J. Chem. Phys.* **1955**, *23*, 1833, 1841, 2338, 2343; **1962**, *32*, 326.
 (5) Politzer, P.; Mulliken, R. S. *J. Chem. Phys.* **1971**, *55*, 5135.
 (6) King, W. T.; Mast, G. B.; Blanchette, P. P. *J. Chem. Phys.* **1972**, *56*, 4440.
 (7) King, W. T.; Mast, G. B. *J. Phys. Chem.* **1976**, *80*, 2521.
 (8) *Gaussian 92*, Revision C; Frisch, M. J.; Trucks, G. W.; Head-Gordon, M.; Gill, P. M. W.; Wong, M. W.; Foresman, J. B.; Johnson, B. G.; Schlegel, H. B.; Robb, M. A.; Replogle, E. S.; Gomperts, R.; Andres, J. L.; Raghavachari, K.; Binkley, J. S.; Gonzalez, C.; Martin, R. L.; Fox, D. J.; Defrees, D. J.; Baker, J.; Stewart, J. J. P.; Pople, J. A. Gaussian Inc., Pittsburgh, PA, 1992.
 (9) Raghavachari, K.; Pople, J. A. *Int. J. Quantum Chem.* **1981**, *20*, 1067.
 (10) Biarge, J. F.; Herranz, J.; Morcillo, J. *An. Real Soc. Esp. Fis. Quim.* **1961**, *A57*, 81.
 (11) Gussoni, M.; Castiglioni, C.; Ramos, M. N.; Rui, M.; Zerbi, G. *J. Mol. Struct.* **1990**, *224*, 445.
 (12) Rupprecht, A. *J. Mol. Spectrosc.* **1981**, *89*, 356.
 (13) Person, W. B.; Newton, J. H. *J. Chem. Phys.* **1974**, *61*, 1040.
 (14) Cioslowski, J. *Phys. Rev. Lett.* **1989**, *62*, 1489.
 (15) Sambe, H. *J. Chem. Phys.* **1974**, *58*, 4779.
 (16) King, W. T. In *Vibrational Intensities in Infrared and Raman Spectroscopy*; Person, W. B., Zerbi, G., Eds.; Elsevier: Amsterdam, 1982; Chap. 6.
 (17) Cioslowski, J. *J. Am. Chem. Soc.* **1989**, *111*, 8333.
 (18) Cioslowski, J.; Hay, P. J.; Ritchie, J. P. *J. Phys. Chem.* **1990**, *94*, 148.
 (19) Wiberg, K. B.; Rablen, P. R. *J. Comput. Chem.* **1993**, *14*, 1504.
 (20) Person, W. B.; KuBulat, K. *J. Mol. Struct.* **1988**, *173*, 357.
 (21) Person, W. B. In *Vibrational Intensities in Infrared and Raman Spectroscopy*; Person, W. B., Zerbi, G., Eds.; Elsevier: Amsterdam, 1982; Chap. 7. Galabov, B.; Dudev, T. *Vibrational Intensities. In Vibrational Spectra and Structure*; Durig, J. R., Ed.; Elsevier: New York, 1996; Vol. 22, Chapter 4.
 (22) Crawford, B. Jr. *J. Chem. Phys.* **1952**, *20*, 977.
 (23) Gordon, R. G. *J. Chem. Phys.* **1963**, *38*, 1724.
 (24) Overend, J. In *Infrared Spectroscopy and Molecular Structure*; Davies, M., Ed.; Elsevier Science: New York, 1963; Chapter 10.
 (25) Crawford, B., Jr. *J. Chem. Phys.* **1958**, *29*, 1042.
 (26) Kuhn, W. Z. *Physik* **1925**, *33*, 408.
 (27) Thomas, W. *Naturwissenschaften* **1925**, *13*, 627.
 (28) Heisenberg, W. Z. *Physik* **1925**, *33*, 879.
 (29) Kondo, S.; Saeki, S. *J. Chem. Phys.* **1981**, *74*, 6603.
 (30) Kondo, S.; Nakanaga, T.; Saeki, S. *J. Chem. Phys.* **1980**, *73*, 5409.
 (31) Newton, J. H.; Person, W. B. *J. Chem. Phys.* **1976**, *64*, 3036.
 (32) Ferreira, M. M. C.; Neto, B. B.; Bruns, R. E. *J. Phys. Chem.* **1989**, *93*, 2957.
 (33) Ferreira, M. M. C.; Suto, E. *J. Phys. Chem.* **1992**, *96*, 8844.
 (34) Prasad, P. L.; Singh, S. *J. Chem. Phys.* **1977**, *66*, 1621.
 (35) Wiberg, K. B.; Murcko, M. A.; Laidig, K. E.; MacDougall, P. J. *J. Phys. Chem.* **1990**, *94*, 6956.
 (36) Engvist, O.; Karlström, G.; Widmark, P.-O. *Chem. Phys. Lett.* **1977**, *265*, 19.
 (37) Craig, N. C.; Chen, A.; Suh, K. H.; Klee, S.; Mellau, G. C.; Winnewisser, B. P.; Winnewisser, M. *J. Am. Chem. Soc.* **1997**, *119*, 4789.
 (38) Papasavva, S.; Tai, S.; Illinger, K. H.; Kenny, J. E. *J. Geophys. Res.* **1997**, *102*, 13643.
 (39) Aleksanyan, V. T.; Samvelyan, S. Kh. In *Vibrational Spectra and Structure*; Durig, J. R., Ed.; Elsevier: New York, 1985; Vol. 14, Chap. 5.
 (40) Ramos, M. N.; Fausto, R.; Teixeira-Dias, J. J. C.; Castiglioni, C.; Gussoni, M.; Zerbi, G. *J. Mol. Struct.* **1991**, *248*, 281.
 (41) Goodwin, A. R. H.; Morrison, G.; *J. Phys. Chem.* **1992**, *96*, 5521.
 (42) Roehl, C. M.; Boglu, D.; Bruehl, C.; Moortgat, G. K. *Geophys. Res. Lett.* **1995**, *22*, 815.